Available online at www.sciencedirect.com
SCIENCE DIRECT®
Applied Thermal Engineering 25 (2005) 173–182
APPLIED THERMAL ENGINEERING
www.elsevier.com/locate/apthermeng

Development of a plate-pin fin heat sink and its performance comparisons with a plate fin heat sink

Xiaoling Yu *, Jianmei Feng, Quanke Feng, Qiuwang Wang

School of Energy and Power Engineering, Xi'an Jiaotong University, Xi'an 710049, China

Received 17 March 2004; accepted 20 June 2004
Available online 20 August 2004

Abstract

Based on plate fin heat sinks (PFHSs), a new type of plate-pin fin heat sink (PPFHS) is constructed, which is composed of a PFHS and some columnar pins staggered between plate fins. Numerical simulations and some experiments were performed to compare thermal performances of these two types of heat sinks. The simulation results showed that thermal resistance of a PPFHS was about 30% lower than that of a PFHS used to construct the PPFHS under the condition of equal wind velocity. Another obvious advantage of PPFHSs is that users can change an existing unsuitable PFHS into a required PPFHS by themselves to achieve better air-cooling results.

Keywords: Heat sink; Heat transfer; Thermal resistance; Electronic device cooling

1. Introduction

Plate fin heat sinks (PFHSs) are widely used in electronic equipment cooling because of their many advantages, such as easy machining, simple structure, and low cost. Various forms of PFHSs are manufactured and supplied to markets in large quantity, and they can achieve excellent solutions for many thermal issues in electronic equipments. Many publications studied the

* Corresponding author. Tel.: +86 29 2675220; fax: +86 29 2668724.
E-mail address: xlingyu@mailst.xjtu.edu.cn (X. Yu).

1359-4311/$ - see front matter © 2004 Elsevier Ltd. All rights reserved.
doi:10.1016/j.applthermaleng.2004.06.016

optimization of the PFHS and attempted to define general rules for optimizing it [1–3]. All these researches focused on optimization of design parameters and the operating condition of a cooling system. However, there exists an intrinsic shortcoming in structures of PFHSs, i.e. parallel plate fins make airflows passing through heat sinks smoother. This is undesirable for enhancing heat transfer performances of heat sinks. Sometimes the existing PFHSs cannot satisfy cooling requirements of some electronic products in small quantity, and it will take some trouble for the users to find proper PFHSs. In this case, it will be helpful to reduce the cost of the total electronic device, if users can modify the heat sink structure and improve heat transfer performance of it by themselves.

Based on the reasons mentioned above, an idea of how to make the flow in a PFHS more turbulent and heat transfer performance of the heat sink stronger was formed, and a plate-pin fin heat sink (PPFHS) was constructed from an existing PFHS. Thermal performances of the PPFHS will be compared with that of the PFHS in this paper.

2. Numerical analysis

The schematic diagrams of a PFHS and a PPFHS composed of the PFHS and some columnar pins are shown respectively in Fig. 1a and b. Geometric parameters of them are listed in Table 1.

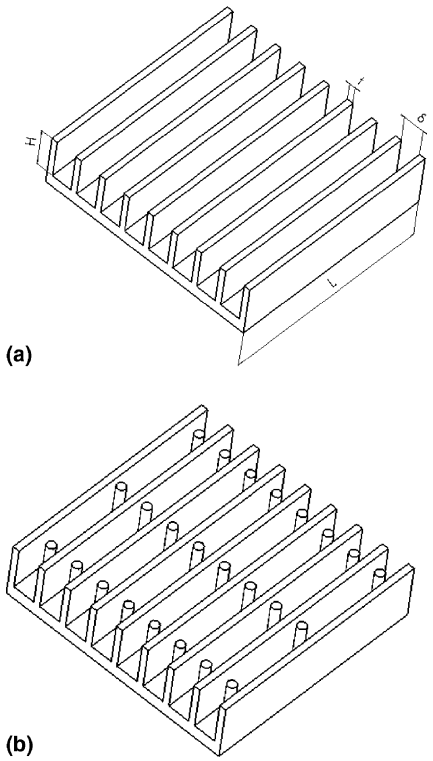

Fig. 1. Schematic diagrams of heat sinks: (a) plate fin heat sink; (b) plate-pin fin heat sink.

Table 1
Geometry parameters of heat sinks

Fin length, L (mm)	Fin height, H (mm)	Fin number, N	Fin thickness, t (mm)	Pin diameter, D (mm)
51	10	9	1.5	2

In the PPFHS, the center distance of two neighbor pins is set as $10D$ (D is the pin diameter) in flow direction, and the nearest distance between the pin center and fin wall is set as $1D$ [4].

The computation domain and the coordinate system are illustrated in Fig. 2. A flow passage in each heat sink was selected as the computation domains. In order to guarantee no back flow in outlets, the computation domains cover $1L$ downstream of the fin arrays in negative z direction. Two sides of the computation domains in x direction are the center planes (symmetry planes) of plate fins.

The flow is assumed as three-dimensional, turbulent, incompressible, and steady flow. Buoyancy and radiation heat transfer effects are negligible. Thermodynamic properties are assumed to be constant. The k–ε turbulence model is used to describe the characteristics of air flow through heat sinks [5]. Assuming that the flow variables can be written in the form $f = \bar{f} + f'$ where $\bar{f}$ is the mean value and f' is a fluctuation about the mean, then the continuity and momentum equation can be written as

$$\frac{\partial}{\partial x_j}(\rho \bar{u}_j) = 0 \tag{1}$$

$$\frac{\partial}{\partial x_j}(\rho \bar{u}_j \bar{u}_i) = -\frac{\partial \bar{p}}{\partial x_i} + \frac{\partial}{\partial x_j}\left(\mu \frac{\partial \bar{u}_i}{\partial x_j} + \tau_{ij}\right) \tag{2}$$

where τ_{ij} is the Reynolds stress term given by

$$\tau_{ij} = \mu_t \left(\frac{\partial \bar{u}_i}{\partial x_j} + \frac{\partial \bar{u}_j}{\partial x_i}\right) - \frac{2}{3}\rho \delta_{ij} k \tag{3}$$

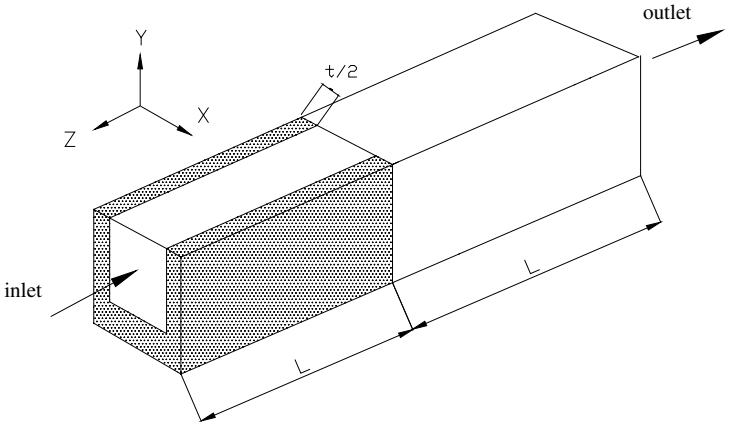

Fig. 2. Computation domain.

where μ_t is the turbulent viscosity and $k = \frac{1}{2}(\overline{u'^2} + \overline{v'^2} + \overline{w'^2})$ is the turbulent kinetic energy. Eq. (3) introduces two unknowns (μ_t and k), which require two equations for closure. For high Reynolds number flows the turbulent viscosity can be represented as

$$\mu_t = \rho C_\mu \frac{k^2}{\varepsilon} \tag{4}$$

where C_μ is a constant and ε is the dissipation rate of energy. The closure equations used to evaluate the turbulent viscosity and energy dissipation rate take the form

$$\frac{\partial}{\partial x_j}(\rho \bar{u}_j k) = \frac{\partial}{\partial x_j}\left[\left(\mu + \frac{\mu_t}{\sigma_k}\right)\frac{\partial k}{\partial x_j}\right] + \mu_t\left(\frac{\partial \bar{u}_i}{\partial x_j} + \frac{\partial \bar{u}_j}{\partial x_i}\right)\cdot\frac{\partial \bar{u}_i}{\partial x_j} - \rho\varepsilon \tag{5}$$

$$\frac{\partial}{\partial x_j}(\rho \bar{u}_j \varepsilon) = \frac{\partial}{\partial x_j}\left[\left(\mu + \frac{\mu_t}{\sigma_\varepsilon}\right)\frac{\partial \varepsilon}{\partial x_j}\right] + C_1\frac{\varepsilon}{k}\mu_t\left(\frac{\partial \bar{u}_i}{\partial x_j} + \frac{\partial \bar{u}_j}{\partial x_i}\right)\cdot\frac{\partial \bar{u}_i}{\partial x_j} - C_2\rho\frac{\varepsilon^2}{k} \tag{6}$$

For the k–ε model, the constant terms take the values

$$C_\mu = 0.09 \quad C_1 = 1.44 \quad C_2 = 1.92 \quad \sigma_k = 1.0 \quad \sigma_\varepsilon = 1.3 \tag{7}$$

The energy equation solved for the fluid flow is

$$\bar{u}_i\frac{\partial \bar{T}}{\partial x_i} = \frac{\partial}{\partial x_i}\left(\Gamma\frac{\partial \bar{T}}{\partial x_i} - \overline{T'u'}\right) \tag{8}$$

where Γ is diffusion coefficient of air. The energy equation solving conduction heat transfer within the heat sink is

$$\frac{\partial}{\partial x_i}\left(\lambda_s\frac{\partial T_s}{\partial x_i}\right) + \dot{q} = 0 \tag{9}$$

where $\dot{q}$ is the heat generated per unit volume of the heat sink, λ_s is the heat sink thermal conductivity and T_s is the temperature within the heat sink.

The solution algorithm used in this paper is the SIMPLE method described in [5]. The discrete schemes of convection items are QUICK scheme with three-order precision.

The flow velocity, k and ε were specified at the inlet, and they were assumed to have zero gradient in the z direction at the outlet. Non-slip boundary condition for velocity was provided on walls. The standard wall functions were used to treat near wall domain. Uniform heat flux condition was applied on the bottom surface of fin base. On the symmetric planes, adiabatic conditions were provided to the velocity u, k, and ε. Grid structures were fine enough to give results independent of grids. Properties of the working fluid are the same as those of air at 294 K, and the material of heat sinks is aluminum with thermal conductivity of 202 W/(mK).

3. Experiments

Jonsson and Moshfegh performed experiments on a group of PFHSs in a wind tunnel [6]. One of PFHSs had the same geometric parameters as the one in Fig. 1a. The wind tunnel height was 10

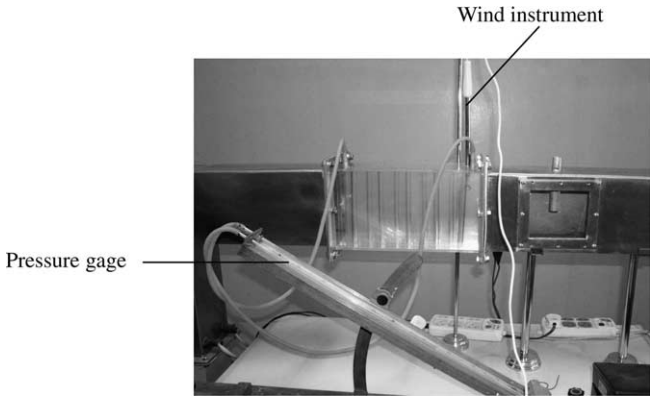

Fig. 3. Experiment device measuring pressure drops over the PPFHS model.

mm, and the wind tunnel width was 63 mm when the PFHS was shrouded. The base of the PFHS was heated uniformly with a heat load of 10 W. When airflows passing through passages of the heat sink were turbulent, wind velocities through passages of the heat sink were 6.5, 8.0, 10.0 and 12.2 m/s respectively. The air temperature at the wind tunnel inlet was held at approximately 21 °C during the experiments.

In order to verify the thermal model of the PPFHS, pressure drops over a scaled PPFHS model were measured under different wind velocities. The size of the PPFHS model is 5.6 times as much as the size of the PPFHS used in computation. The columnar pins were staggered in two flow passages of the model. The center distances of two neighbor pins were set as $5D$ in flow direction. The pressure drop over the model was measured using two pressure taps positioned 30 mm upstream and downstream respectively of a passage with staggered pins. The taps were connected to a tilter U type pressure gage. The wind velocity changed from 1.5 to 4.5 m/s was measured by a thermal bulb type wind instrument. The experiment device is shown in Fig. 3.

4. Results and discussion

4.1. Experiment and simulation results

The thermal resistance of the heat sink, R_{th}, can be defined by

$$R_{th} = \frac{\Delta T}{Q} \tag{10}$$

where ΔT is temperature difference between the highest temperature on the fin base and the ambient air temperature, and Q is heat dissipation power applied on the fin base.

Both simulation results and Jonsson and Moshfegh's experiment results for thermal resistances and pressure drops of the PFHS are plotted in Fig. 4 a and b respectively. As can be seen in these figures, agreements of experiment data and simulation data for both thermal resistances and pressure drops are within ±10%.

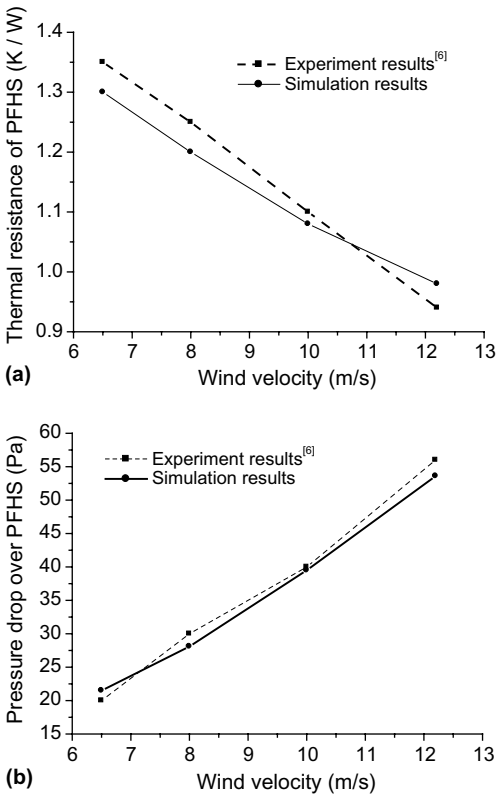

Fig. 4. Experiment and simulation results for the PFHS: (a) thermal resistances; (b) pressure drops.

Experiment and simulation results of pressure drops over the PPFHS model are listed in Table 2. The simulation results become lower than the experiment results as the wind velocity increasing. The reason is not quite clear to the authors. A possible explanation is that the thermal bulb of the wind instrument is not quite vertical to the air flow direction because of air force effect, and so the measured wind velocity is lower than the real value. Generally, The error between simulation results and experiment results is less than 20%. This indicates that simulation results of the PPFHS are reasonable.

4.2. Comprehensive performance comparison between PFHS and PPFHS

The thermal resistances and pressure drops of the two types of heat sinks under different wind velocities are shown in Fig. 5a and b respectively. From the figures, it is seen that thermal resistance of the PPFHS is about 30% lower, and pressure drop of it is much higher than that of the PFHS under the condition of equal wind velocity. As the pressure drop is directly proportional to the pumping power required to move the cooling air through the heat sink [7], a synthetical comparison should be made between these two types of heat sinks. A profit factor J defined by Eq. (11) is introduced to represent the synthetical performance of a heat sink.

Table 2
Pressure drops over the PPFHS model

Wind velocity (m/s)	Pressure drop over the PPFHS model (Pa)		
	Simulation results	Experiment results	Error
1.5	11.0	10	10%
2.0	19.2	20	4%
2.5	29.7	35	15%
2.8	37.0	45	18%
3.5	62.4	75	17%
4.5	110.5	130	15%

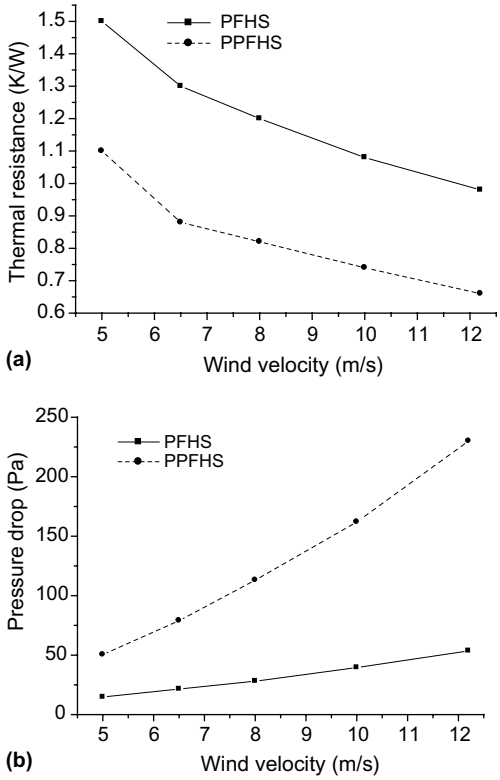

Fig. 5. Thermal resistances (a) and pressure drops (b) of two types of heat sinks vs. wind velocities.

$$J = Q/P \tag{11}$$

where P given by Eq. (12) is the pumping power required to propel a mass flow $\dot{m}$ through a pressure drop Δp [8].

$$P = (\dot{m}/\rho)\Delta p = wA_p\Delta p \tag{12}$$

$$A_p = H \cdot \delta \cdot (N - 1) \tag{13}$$

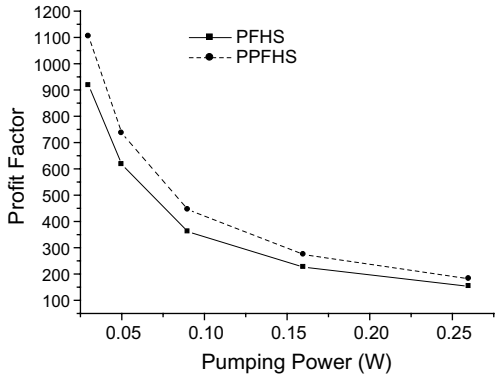

Fig. 6. Profit factors of two types of heat sinks vs. pumping powers.

N is the number of plate fins. When a heat sink is used in natural convection, a pumping power is equal to zero, and therefore the value of profit factor is equal to ∞. Fig. 6 is profit factor curves of the two heat sinks when temperatures on bottom surfaces of two heat sink bases $\bar{t}_{hs}$ remain 60 °C. It shows that the profit factor decreases as the pumping power increases, and the profit factor of the PPFHS is about 20% higher than that of the PFHS with the same pumping power. This indicates that the PPFHS needs less pumping power than the PFHS when the heat dissipation power is the same for the two types of heat sinks. Therefore, adopting the PPFHS can make the volume of air-cooling system smaller.

In order to further study benefit of the PPFHS, the thermal performance of the PPFHS is compared with an optimized PFHS. Both of structures have the same dimensions of plate fins and fin bases. The optimization process of the PFHS is proceeded by changing fin number from 7 to 17. Fig. 7 shows the relations between thermal resistances of the heat sinks and the pumping powers. It can be found that there exists an optimum fin number for a given thermal resistance. For example, the optimum fin number is 11 for thermal resistance of 1.0 K/W and 13 for thermal resistance of 0.8 K/W respectively. For thermal resistance of 1.0 K/W, the PPFHS needs nearly the same

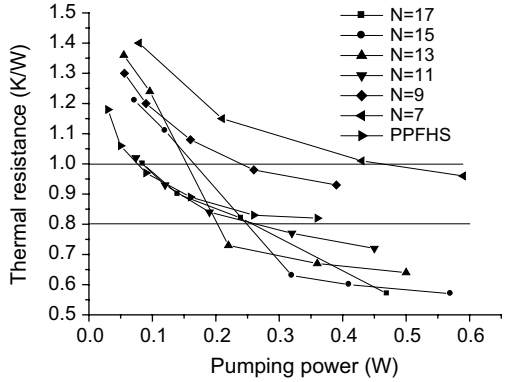

Fig. 7. Thermal resistances of PFHSs with different fin numbers vs. pumping powers.

pumping power as the optimum PFHS. Actually, the PPFHS can be optimized as well as the PFHS. But no more details are given in this paper and this work will be discussed in future publications.

The process of constructing a PPFHS from a PFHS is not very complex for users. A PPFHS can be constructed by drilling holes in flow passages of a PFHS and inserting columnar pins into these holes. If drilling holes will make the bottom surface of fin base rough and irregular, the bottom surface should be grinded to keep it deadly smooth after inserting pins.

4.3. Application of PPFHSs

As mentioned above, when heating powers are uniform on bottom surfaces of fin bases, thermal resistances of PPFHSs are always lower than that of PFHSs used to construct the PPFHSs under the condition of equal pumping powers. However, heating powers are often center concentrated on fin bases in real engineering applications, for example, in central processor unit (CPU) cooling. PPFHSs can be adopted more flexibly than PFHSs when heat sources are not uniform but concentrative. Pins in PPFHSs can be arranged closer in heat source areas, and pin numbers can be adjusted according to cooling condition. Heat transfer performance of a PPFHS used for a CPU cooling will be discussed here. The geometry parameters of a PFHS and a copper spreader are described in reference [9]. The optimum geometry parameters for fin thickness and fin gap are 0.8 and 2.0 mm respectively in the PFHS [9]. The sizes of plate fins and fin base of the PPFHS are the same as that of the PFHS, and the fin gap is assumed as 2.5 mm in the PPFHS. The columnar pins with diameter of 0.8 mm are concentrated in the copper spreader area. The center distance of them in the flow direction is set as 8 mm, and the nearest distance between the pin center and plate fin wall is set as 0.8 mm. Because the heat source is center located on the fin base, the computation domain is the half of the total cooling system, which includes the copper spreader and the heat sink. The CPU power is expected up to 100 W in the near future, and therefore heat load of 100 W is applied in the die area uniformly. The ambient air temperature is assumed as 40 °C . The temperature on the surface of CPU, T_{CPU}, changed with the pumping power is plotted in Fig. 8. T_{CPU} should be limited as 85 °C in real application case. The figure shows that the PPFHS has the same heat dissipation capacity as the optimized PFHS in the working temperature zone of

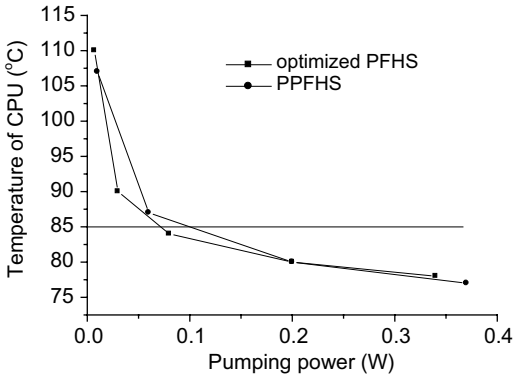

Fig. 8. Temperatures on the surface of CPU vs. pumping powers.

CPU. The PPFHS should get better heat dissipation result after being optimized as well as the PFHS.

5. Conclusion

1. This paper proposed a special solution for improving heat transfer performance of a PFHS by planting some columnar into flow passages of the PFHS to disturb airflows passing through the heat sink. So a PPFHS was constructed.
2. Numerical simulation and experimental results show that the thermal resistance of a PPFHS is 30% lower than that of a PFHS used to construct the PPFHS with the same blowing velocity, and the profit factor of the former is about 20% higher than that of the latter with the same pumping power.
3. Users can get various forms of PPFHSs by themselves from an existing PFHS through planting columnar pins with different numbers or different geometry parameters, and so get various PPFHSs with different cooling performances for their special requirements.

References

[1] J.R. Culham, Y.S. Muzychka, Optimization of plate fin heat sinks using entropy generation minimization, IEEE Transactions on Components and Packaging Technologies 24 (2) (2001) 159–165.
[2] M. Iyengar, A. Bar-Cohen, Least-energy optimization of forced convection plate-fin heat sinks, IEEE Transactions on Components and Packaging Technologies 26 (1) (2003) 62–70.
[3] Andrea de Lieto Vollaro, S. Grignaffini, F. Gugliermetti, Optimum design of vertical rectangular fin arrays, International Journal of Thermal Science 38 (1999) 525–529.
[4] X.L. Yu, Q.K. Feng, Q.P. Liu, Research on the heat transfer and flow performance of a composite heat sink, Journal of Xi'an Jiaotong University 37 (7) (2003) 670–673 (in Chinese).
[5] W.Q. Tao, Numerical Heat Transfer, second ed., Publishing Company of Xi'an Jiaotong University, Xi'an, 2001 (in Chinese).
[6] H. Jonsson, B. Moshfegh, Modeling of the thermal and hydraulic performance of plate fin, strip fin, and pin fin heat sinks—influence of flow by pass, IEEE Transactions on Components and Packaging Technologies 24 (2) (2001) 142–149.
[7] K.A. Moores, Y.K. Joshi, Numerical and experimental characterization of a liquid cooled AlSiC power electronics base plate with integral pin fins, in: The Seventh Intersociety Conference on Thermal and Thermo-mechanical Phenomena in Electronic Systems, Las Vegas, Nevada, vol. 2, 2000, pp. 385–390.
[8] E.M. Sparrow, J.W. Ramsey, C.A.C. Altemani, Experiments on in-line pin fin arrays and performance comparisons with staggered arrays, Journal of Heat Transfer, Transactions of the ASME 102 (1980) 44–50.
[9] M. Saini, R.L. Webb, Heat rejection limits of air cooled plane fin heat sinks for computer cooling, Part A: IEEE Transactions on Packaging Technologies 26 (1) (2003) 71–79.